http://ansinet.com/itj

ITJ

ISSN 1812-5638

INFORMATION TECHNOLOGY JOURNAL

ANSInet
Asian Network for Scientific Information
308 Lasani Town, Sargodha Road, Faisalabad - Pakistan

Information Technology Journal 7 (1): 205-209, 2008
ISSN 1812-5638

Automatic Classification of Focal Lesions in Ultrasound Liver Images Using Combined Texture Features

S. Poonguzhali and G. Ravindran
Center for Medical Electronics, College of Engineering, Guindy, Anna University,
Chennai-600 025, Tamil Nadu, India

Abstract: In this study, the ultrasound liver images are studied to build a computer-aided automatic early detection system for the identification of cysts, tumors and cancers by analyzing their unique echo texture patterns using a custom designed back propagation neural network classifier. The texture features are extracted using various statistical and spectral methods. Then the optimal feature selection process is carried out manually to select the best discriminating features from the extracted texture parameters. Then the neural network has been designed and the optimal neural network parameters have been selected to increase the classifier performance.

Key words: Texture, image analysis, feature extraction, classification, neural networks, ultrasound imaging

INTRODUCTION

Diagnostic ultrasound is a useful clinical tool for imaging the human soft tissues. It enables the operator to select the right image plane to display the pathological anatomy accurately in the organs like the liver, kidney, pancreas etc. (Raeth *et al*., 1985). Its main advantage is that this imaging modality is non-radiological and non-invasive (Sherlock and Dooley, 1993). Presently the doctors identify abnormalities from their unique echo texture patterns by visual interpretation (Wells, 1982).

The number of people especially males infected with liver abnormalities has grown enormously in Asian countries. Especially the occurrence of the focal diseases like cysts, tumors and primary cancers are frequent and if left undetected at an early stage chances of fatality is high (Lee *et al*., 2003). Hence building a computer aided system for preliminary diagnosis and to detect such diseases is under research.

The ultrasound echo texture analysis is the preferred method to analyze the Region of Interest (ROI) as the diseased portion exhibits a different texture from the normal liver surface (Tuceyran *et al*., 1993). In the case of Focal lesions, the infected region is very small in terms of area and volume. The surrounding liver tissues exhibit a normal texture thereby posing difficulty to diagnose.

Books and literatures on diagnostic ultrasound define the echo patterns of the cysts as completely homogeneous in texture and capsular in structure, the hemangiomas (benign tumor) as slightly inhomogeneous, ring shaped, hyper echoic and the metastases (secondary malignant tumors) as irregular and hypo echoic. These facts are useful for differentiating these ROI into their respective classes by texture analysis. In medical image processing, texture analysis means translating the echo texture information into mathematical parameters by using various texture model algorithms.

The most difficult aspect is to define a unique set of meaningful features, as there are many methods available. Tuceyran and Jain (1993) classified the texture analysis methods as statistical, structural, model based and spectral methods. On reviewing the various models of texture, statistical inter pixel relationship matrixes like Grey Level Co-occurrence Matrix (GLCM) and Grey-level Run-length Matrices (GLRLM), Laws and Gabor wavelet based spectral filters (Ahmadian *et al*., 2004) were more preferred for texture description (Wu *et al*., 1992; Sujana *et al*., 1996; Poonguzhali and Ravindran, 2006).

Some of these algorithms have been tested on Computed Tomographic (CT) images, which are of higher contrast than ultrasound images (Mougiakakou *et al*., 2003). But as the ultrasound imaging modality offers the undisputed advantage of being non-invasive, low cost and non-radiological despite low contrast, more research has been initiated in this field.

Thus, in this study, the possibilities of an automatic classification of ultrasonic liver images by employing a combined set of statistical and spectral texture parameters are explored. The combined features are used to classify these images into four classes-Normal, Cyst, Benign and

Corresponding Author: S. Poonguzhali, Center for Medical Electronics, College of Engineering, Guindy, Anna University, Chennai-600 025, Tamil Nadu, India

Malignant masses. Designing a classifier for texture analysis problems based on methods like Linear Discriminant Analysis (LDA), statistical Bayesian classifier, K nearest neighbor etc has been discussed in earlier study (Poonguzhali and Ravindran, 2007).

For multi class problem, an efficient classifier is needed. Hence a supervised learning classifier such as an artificial neural network can be employed. Networks such as Multi layer perception have been used for medical applications like image compression and pattern association (Yoshida *et al*., 2003). Since 1990's, the back Propagation Based Neural Network (BPN) has been efficiently used for medical image processing and in texture based tissue characterization in images of breast, liver etc. (Sujana *et al*., 1996). Hence the usage of BPN for automatic classification of focal liver lesions is described in this study.

MATERIALS AND METHODS

Image acquisition: In this study, the liver images are collected from hospital on various patients taken with ATL HDI 5000 ultrasound machine using curvilinear and sector transducer array of frequency 4 MHZ under similar imaging conditions. The images are grey scale images. The selected images for test are histo-pathologically tested and the radiologists have confirmed the presence of the disease.

The focal lesions like cysts and tumors occur alone or in multiple numbers and are generally of diameter less than 10 cm which could be represented as a small region of grid size 80×80 pixels maximum. Thus the abnormal region is suitably segmented and from this region a sub-image of size 10×10 pixels with 8-bit resolution is chosen for accurate analysis. This reduces the number of false positives in final classification.

FEATURE EXTRACTION

The following four feature selection methods were more preferred for texture description. Hence these features are extracted.

Grey level co-occurrence matrix based statistical texture features: The second order image histogram referred as the Grey Level Co-occurrence Matrix (GLCM) of an image offers greater information about the inter-pixel relationship, periodicity and spatial grey level dependencies. This matrix is a source of 14 meaningful texture descriptors. Previous works in focal lesion segmentation and classification have used the energy and entropy features from this matrix. For the sub-image 4 GLCM matrices are formed with inter-pixel distance equal to 1 varying angle θ in steps of 45° clockwise up to 180° to get a complete description of the sub-image.

Grey level run length matrix based statistical texture features: The grey level run length matrix is another method of extracting the higher order statistics of the texture of the image and has been a major descriptor of the regularity and periodicity of the texture pattern. The Grey Level Run Length Matrix (GLRLM) is a 2D matrix in which each element $p(i,j/\theta)$ gives the total number of consecutive runs of length j at grey level i in the direction θ. From this matrix almost 11 scalar parameters can be computed which analyses the image texture in more detail.

Law's spectral texture features: Law's 1D kernels are popular analysis tools for classifying the different texture patterns based on regularity homogeneity. A number of 2D masks are generated by convolving five 1D kernels with each other. Each of these 1D kernels performs local averaging, edge detection and spot detection and wave detection on the sub-image. These 2D masks are convolved with the image and the horizontal energy function of the filtered image is used as a texture feature after normalization.

Gabor Wavelet's based spectral texture features: Ahamedian *et al*. (2004) suggested that the Gabor Transform coefficients reveal the localized frequency distribution of a signal or an image. Its frequency response is Gaussian in shape and the center frequency of each filter was selected to correspond to a peak in the texture power spectrum. The images are filtered using the Gabor filter bank and the first order mean is extracted to capture the texture homogeneity. 24 Gabor filters of window size 10×10 formed at 4 scales and 6 orientations are applied on the sub-image to extract 24 such Gabor means.

COMBINED TEXTURE FEATURES

Each feature extraction method corresponds to number of texture feature descriptors, some being redundant. This data includes the possibilities of misclassification. Hence a manual search routine is conducted on the entire data set and the best discriminating features are selected (Table 1).

The GLCM based features energy, entropy and the spectral energy features using LAWS are high for the cystic lesion as they are the most homogeneous and regular patterns (Table 1). Instead the

Table 1: Optimal features for selection

	Feature values			
Optimal features	Normal	Cyst	Benign	Metastases
GLCM-energy ($\times 10^2$)	7.5000±0.125	13.6000±0.170	2.7300±0.820	4.050±0.250
GLCM-entropy ($\times 10^2$)	1.4900±0.040	2.8800±0.080	0.6300±0.050	1.080±0.016
GLRLM-long run low grey-level emphasis	0.7500±0.016	3.4000±0.230	0.2820±0.0093	0.531±0.032
GLRLM-long run high grey-level emphasis ($\times 10^2$)	0.7160±0.030	0.5700±0.055	2.8220±0.270	1.250±0.029
LAWS-EE mask	0.0120±0.0015	0.0524±0.0068	0.0204±0.0015	0.018±0.0063
LAWS-EL mask	0.0690±0.006	0.2240±0.0164	0.0950±0.006	0.018±0.0517
Gabor mean (Scale 2 Orientation 0)	0.9930±0.400	0.4018±0.202	2.3900±1.106	1.290±0.620
Gabor mean (Scale 3 Orientation 0)	0.2661±0.040	0.1836±0.101	0.8980±0.4012	0.594±0.170

Gabor mean is very low for homogeneous region such as cyst and high for benign lesion. Similarly from the GLRM features the grey level distributions at different run lengths are measured. The long run high grey level emphasis captures the inhomogeneous nature of the benign lesions.

The lesion's texture information holds the deviation from the normal texture parameter values in each of the class. These features are combined into a single texture parameter vector after suitable scaling for further classification.

Experimentation: Automatic pattern classification is carried out using an artificial neural network based classifier (Haykin, 2001). The neural network based classifier is a supervised classifier, which can take in multiple inputs, train them and classify accordingly (Fig. 1). The neural network for classifying the lesions is simulated using the neural network toolbox function available in MATLAB 6.5.

The network has 8 input nodes and 4 output nodes with the following target mapping -'1000' for normal liver, '0100' for cyst, '0010' for benign and '0001' for malignant metastases. The output of the neural network is mapped with the target using competitive transfer function that produces a 1 for the winning neuron in the output node there by deciding the output class. All the input parameters are scaled suitably so as to avoid the bias caused by unbalanced features. The tan-sigmoid differential activation function is used as transfer function for the network layers.

The neural network parameters such as training algorithm, number of hidden layers, learning rate and momentum constant are generalized for the network by repeated analysis on the basis of minimum execution time, number of epochs to train the network and reaching the minimum sum squared error. Generally for pattern recognition problems minimum two hidden layers are necessary for learning the global and local features of the pattern.

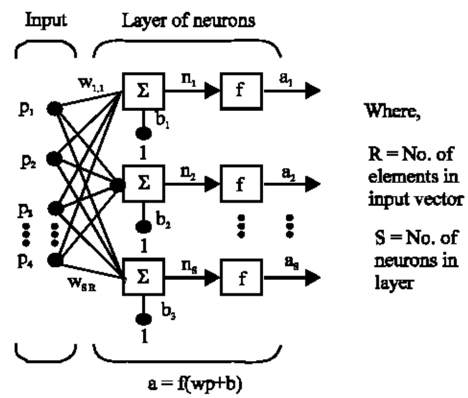

Fig. 1: Neural network architecture

Our network performance is optimal with 2 hidden layers wherein the first layer has 4 hidden units and the second layer has 6 neurons each. The hidden layers and input layers are initialized with random weights and biases lying within the minimum and maximum input scale.

The learning algorithm used in a regular basic back propagation algorithm is steepest descent algorithm with adaptive learning rate and momentum does not necessarily produce faster convergence. Hence we have tried and used a conjugate gradient-based algorithm for training since it achieves faster convergence as it searches for minimum error in conjugate directions. After repeated analysis the learning rate is fixed at 0.01 and the momentum constant is fixed at 0.4.

The performance of the steepest descent algorithm and that of the conjugate gradient algorithm is comparatively studied and the results are shown in Fig. 2.

Figure 2 shows the conjugate gradient algorithm converges to the performance goal with less number of training epochs and less execution time. The network is further tested using jackknife procedure such that 50% of the training set is used for training and the rest is used for testing such that there is no overlap between the data. The network is trained for maximum 5000 learning epochs. The number of sub-images correctly classified into each class is the measure of performance of the classifier.

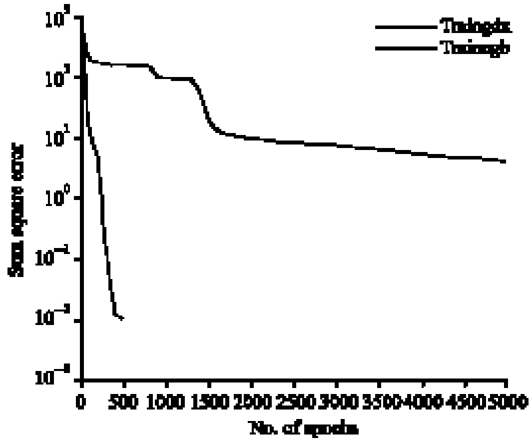

Fig. 2: Comparison of network performance for different training algorithm

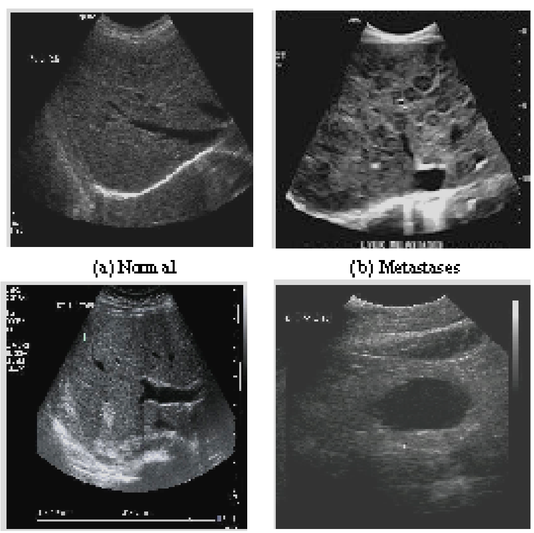

(a) Normal (b) Metastases (c) Benign (d) Cyst

Fig. 3: Ultrasound images used in study

Table 2: Performance of the classifier

Output classes	Rate of correct classification (%)
Normal liver lesion	75
Cystic lesion	94
Benign lesion	81
Malignant lesion	90

RESULTS

In this study, images of each class-normal, cyst, benign and malignant lesion are collected and 30 sub-images from each class are used as the image database. The sample images are shown in Fig. 3. The optimal features are extracted and given as input to the neural network for classification. Table 2 shows that the performance of the classifier is good for cysts since they are the most homogeneous texture and distinct among the four classes.

This classifier also offers better results in identifying the malignant lesion from the surrounding normal region. The benign tumors are misclassified as normal in some cases as their textures are quite similar, the shape and symptoms help the doctors to easily differentiate the benign tumors from the normal parenchyma. The over all accuracy of the classifier is nearly 83% for the liver images in our database.

CONCLUSIONS

The information contained in the ultrasound image is a delineation of the complex interaction between ultrasound waves and tissue components once the standardized imaging procedures have been adopted sonographically for best diagnostic image possible. Thus the accuracy of conventional classification based on clinical b-scan method is limited by recognition of important features and experience of sonographers. In this study a multi-class multi-variant problem like classification of the focal lesions of the liver using ultrasound liver images is automated by the selection of optimal features and back propagation neural network. The initial implementations of the combined texture vector for classifying the liver lesion are promising as it yields better rate of classification. In future, incorporating preprocessing units to eliminate the speckle noises and improving the image quality and contrast will increase the performance further.

ACKNOWLEDGMENT

The authors are grateful to Dr. S. Suresh, Director and Dr.Madhavan, MEDISCAN Systems for providing the ultrasound liver images and the required clinical information.

REFERENCES

Ahmadian, A., A. Mostafa, M.D. Abolhassani and N. Riahi Alam, 2004. A method for texture classification of ultrasonic liver images based on Gabor wavelet. Proc. IEEE-ICSP'04, China, 2: 971-974.

Haykin, S., 2001. Neural Networks. A Comprehensive Study. 2nd Edn., Pearson's Education Inc.

Laws, K.I., 1980. Rapid texture identification. Proceedings of SPIE Image Processing for Missile Guidance, 238: 376-380.

Lee, W.L., Y.C. Chen and K.S. Hsieh, 2003. Ultrasonic liver tissues classification by fractal texture vector based on m-band wavelet transform. IEEE Trans. Med. Imag., 22: 382-392.

Mougiakakou, S. Gr., I. Valavanis, K.S. Nikita, A. Nikita and D. Kelekis, 2003. Characterization of CT liver lesions based on texture features and a multiple neural network classification scheme. Proc. IEEE EMBC, pp: 1287-1290.

Poonguzhali, S. and G. Ravindran, 2006. Performance evaluation of feature extraction methods for classifying liver abnormalities in ultrasound images using neural network. Proceeding of the 28th Annual International Conference of the IEEE EMBS, New York, pp: 4791-4794.

Poonguzhali, S., B. Deepalakshmi and G. Ravindran, 2007. Optimal feature selection and automatic classification of abnormal masses in ultrasound liver images. Proceeding of the IEEE-ICSCN, MIT Campus, Anna University, Chennai, India, pp: 503-506.

Raeth, U., D. Schlaps, B. Limberg, I. Zuna, A. Lorenz, G. van Kaick, W.J. Lorenz and B. Kommerell, 1985. Diagnostic accuracy of computerized B-Scan texture analysis and conventional ultra-sonography in diffuse parenchyma and malignant liver diseases. J. Clin. Ultra., 13: 87-89.

Sherlock, S. and J. Dooley, 1993. Diseases of the Liver and Biliary System. 9th Edn., Blackwell Scientific Publication.

Sujana, H., S. Swarnamani and S. Suresh, 1996. Application of artificial neural networks for the classification of liver lesions by image texture parameters. Ultra. Med. Biol., 22: 1177-1181.

Tuceyran, M. and A.K. Jain, 1993. Texture analysis. Handbook of Pattern Recognition and Computer Vision, 2: 235-276.

Wells, P.N.T., 1982. Scientific Basis of Medical Imaging. William Clowes Limited, Beccles and London.

Wu, C.M., Y.C. Chen and K.S. Hsieh, 1992. Texture features for classification of ultrasonic liver images. IEEE Trans. Med. Imag., 11: 142-152.

Yoshida, H., D.D. Casalino, B. Keserci, A. Coskun, O. Ozturk and A. Savranlar, 2003. Wavelet packet based texture analysis for differentiation between benign and malignant liver tumors in ultrasound images. J. Phys. Med. Biol. Inst. Phys. Publ., 48: 3735-3753.